

Cathodic Evolution of Hydrogen at Pd-Modified Carbon Fibre in 0.1 M NaOH

Boguslaw Pierozynski^{1,*}, Ireneusz M. Kowalski², Tomasz Mikolajczyk¹ and Marcin Turemko¹

¹ Department of Chemistry, Faculty of Environmental Management and Agriculture, University of Warmia and Mazury in Olsztyn, Plac Lodzki 4, 10-957 Olsztyn, Poland

² Department of Rehabilitation, Faculty of Medical Sciences, University of Warmia and Mazury in Olsztyn, Zolnierska 14C Street, 10-561 Olsztyn, Poland

*E-mail: bogpierzynski@yahoo.ca

Received: 21 July 2013 / Accepted: 19 August 2013 / Published: 25 September 2013

This work is concerned with an a.c. impedance study of hydrogen evolution reaction (HER), performed on carbon fibre (CF) and Pd-modified carbon fibre 12K tow materials. The HER was examined in 0.1 M NaOH solution for electrochemically oxidized Hexcel 12K AS4C and Pd-modified Hexcel carbon fibre tow samples. Kinetics of the hydrogen evolution reaction were studied at room temperature (and for the temperature range: 23-60 °C), over the cathodic overpotential range: -50 to -1400 mV vs. RHE. The resultant values of charge-transfer resistance, exchange current-density for the HER and other electrochemical parameters for the examined CF materials were derived. Hence, Pd-modification of CF tow material (at *ca.* 1.5 wt.% Pd) dramatically increased the kinetics of the HER, yielding series opportunities for this type of cathode materials in commercial water electrolyzers.

Keywords: carbon fibre; CF; HER; Pd-modification; impedance spectroscopy.

1. INTRODUCTION

One of the most important applications for carbon fibre (CF) based materials is their utilization in electrostatic dissipation (ESD) and electromagnetic interference (EMI) shielding techniques. These technologies cover a number of important industry markets, including: automotive, cell-phone, laptop computer and military industry applications [1-6]. Other examples involve employment of carbon fibre (or similar C-based materials) in preparation of electrochemically active composite catalysts [7-14].

This paper makes an extension of a series of earlier publications [11-14] from this laboratory on kinetic aspects of hydrogen evolution reaction (HER), examined at carbon fibre and nickel-coated carbon fibre (NiCCF) composite materials. Current work primarily constitutes an a.c. impedance study

of the HER, which is performed on Pd-modified carbon fibre (polyacrylonitrile, PAN-based Hexcel 12K AS4C product [15] is a continuous 12K ribbon: 12,000 single filaments of 7 μm diameter each) in 0.1 M NaOH supporting electrolyte. In this sense, current paper could be referred to other HER works, examined on noble metal catalysts (e.g. Pt) or their alloys (see e.g. Refs. 16-24), but for a very large (and greatly modifiable) electrochemically active surface area (an effective length of the 12K tow's entity for 1 cm long tow electrode translates to about 26 cm^2 of the total geometrical surface area exposed to the electrolyte).

2. EXPERIMENTAL

All solutions were prepared by means of a Direct-Q3 UV ultra-pure water purification system from Millipore. Aqueous, 0.1 M NaOH solution was prepared from AESAR, 99.996% NaOH pellets (also, in order to carry-out oxidation pre-treatments to carbon fibre samples). Atmospheric oxygen was eliminated from solution before each electrochemical experiment through bubbling with high-purity argon (Ar 6.0 grade, Linde). In addition, the argon gas flow was kept above the solution upon all impedance measurements.

An electrochemical cell, made all of Pyrex glass, was used during the course of this work. The cell comprised three electrodes: a CF-based working electrode (WE) in a central part, a reversible Pd hydrogen electrode (RHE) as reference and a Pt counter electrode (CE), both placed in separate compartments. Prior to Pd electrodeposition, each CF tow sample was pre-treated (electrooxidized) in 0.1 M NaOH solution, at an anodic current-density of 0.4 mA cm^{-2} for 300 s. Electrodeposition of Pd on CF tow electrodes was carried-out from PdCl_2 (2 g dm^{-3}) solution of pH 1.5, at a cathodic current-density of 0.2 mA cm^{-2} for palladium loadings of ca. 1-2 wt.% Pd (or comparatively at 5.0 mA cm^{-2} for high, ca. 50 wt.% Pd loadings). The palladium RHE was made of a coiled Pd wire (0.5 mm diameter, 99.9% purity, Aldrich) and sealed in soft glass. Before its use, this electrode was cleaned in hot sulphuric acid, followed by cathodic charging with hydrogen in 0.5 M sulphuric acid until H_2 bubbles in the electrolyte were clearly observed. The counter electrode was made of a coiled Pt wire (1.0 mm diameter, 99.9998% purity, Johnson Matthey, Inc.). Prior to its use, the counter electrode was cleaned in hot sulphuric acid. In the same way, before each series of experiments, the electrochemical cell was taken apart and soaked in hot sulphuric acid for at least 3 hours. After having been cooled to about 30 $^\circ\text{C}$, the cell was thoroughly rinsed with Millipore ultra-pure water.

An electrochemical a.c. impedance spectroscopy technique was employed during the course of this work. All measurements were conducted at room temperature (or over the temperature range: 23-60 $^\circ\text{C}$) by means of the *Solartron* 12.608 W Full Electrochemical System, consisting of 1260 frequency response analyzer (FRA) and 1287 electrochemical interface (EI). The FRA's generator provided an output signal of known amplitude (5 mV) and the frequency range was swept between 1.0×10^5 and 0.5×10^{-1} Hz. The instruments were controlled by *ZPlot 2.9* software for Windows from Scribner Associates, Inc. (*Corrware 2.9* software package was used to carry-out a single, cyclic voltammetry experiment, as later shown in Fig. 4). Usually, three impedance measurements were performed at each potential value, independently at three catalyst tow electrodes. Reproducibility of

such-obtained results was typically around 10 to 20% from tow-to-tow. Data analysis was performed with *ZView 2.9* software package, where the impedance spectra were fitted by means of a complex, non-linear, least-squares imittance fitting program, *LEVM 6*, written by J.R. Macdonald [25]. In addition, spectroscopic characterization of Pd-modified CF fibre composites was performed by means of Quanta FEG 250 scanning electron microscope (SEM).

3. RESULTS AND DISCUSSION

3.1. SEM characterization of Pd-modified CF tow electrode

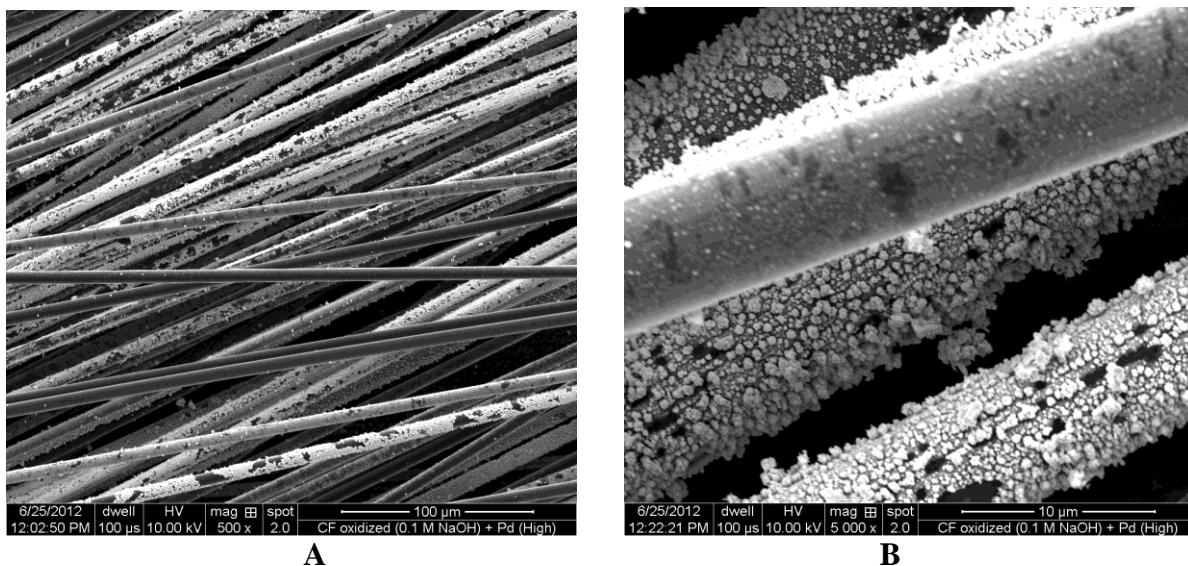


Figure 1. a) SEM micrograph picture of Pd-modified (*ca.* 52 wt.% Pd) CF-oxidized Hexcel 12K AS4C carbon fibre tow sample, taken at 500 magnification. b) As in (a), but taken at 5,000 magnification.

For the HER experiments performed in this work, all Pd-modified CF tow samples contained only *ca.* 1.5 (\pm 0.2) wt.% Pd (derived based on the total charge passed upon Pd electrodeposition per respective mass of CF tow samples), where such metal deposits were practically undetectable (likely due to relatively low electrical conductivity of the CF tow) by the SEM method (respective micrograph pictures are not shown). On the other hand, a sample of Pd-deposited (at *ca.* 50 wt.% Pd), electrooxidized Hexcel 12K CF tow is comparatively shown in SEM micrograph pictures of Figs. 1a and 1b. As can be concluded here, metal deposits obtained via laboratory, batch-type electrodeposition trials (at high Pd loading) are quite irregular and discontinuous throughout the CF_{ox} tow.

3.2. Hydrogen evolution reaction on CF_{ox} and Pd-modified CF_{ox} tow electrodes in 0.1 M NaOH

The a.c. impedance characterization of the HER at electrooxidized and Pd-modified Hexcel 12K AS4C carbon fibre tow electrodes in 0.1 M NaOH is presented in Fig. 2 and Table 1.

Table 1. Electrochemical parameters for the HER, obtained at electrooxidized (in 0.1 M NaOH at $j_a=0.4 \text{ mA cm}^{-2}$) Hexcel 12K CF_{ox.} and Pd-modified Hexcel 12K CF_{ox.} tow electrodes, in contact with 0.1 M NaOH. The results were obtained by fitting the CPE-modified Randles equivalent circuit (see Fig. 3) to the experimentally obtained impedance data (reproducibility usually below 10-15%, $\chi^2 = 6 \times 10^{-4}$ to 2×10^{-3}).

<i>E</i> /mV	<i>R</i> _{ct} /Ω g	<i>C</i> _{dl} /μF g ⁻¹ s ^{φ¹⁻¹}
Hexcel 12K CF _{ox.}		
-600	39.76 ± 2.37	109,210 ± 1,048
-800	8.49 ± 0.15	126,316 ± 1,048
-1000	1.64 ± 0.02	173,684 ± 2,258
-1200	0.52 ± 0.01	223,618 ± 6,395
-1400	0.22 ± 0.00	285,526 ± 14,162
Pd-modified Hexcel 12K CF _{ox.}		
-50	1.03 ± 0.01	182,237 ± 2,916
-100	0.80 ± 0.01	183,553 ± 2,937
-200	0.46 ± 0.00	182,895 ± 4,005
-300	0.29 ± 0.00	180,921 ± 4,414
-400	0.21 ± 0.00	190,059 ± 5,797
-500	0.15 ± 0.00	190,789 ± 6,296
-600	0.12 ± 0.00	190,526 ± 7,049

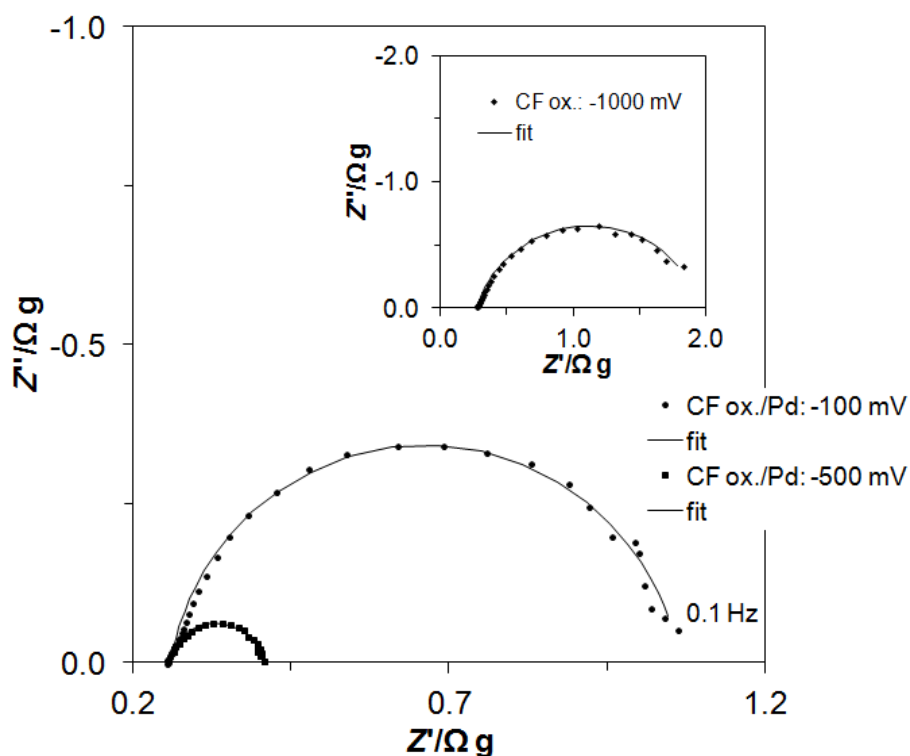


Figure 2. Complex-plane impedance plots for Hexcel 12K AS4C CF (inset) and Pd-modified CF tow electrodes in contact with 0.1 M NaOH, recorded at room temperature for the stated potential values (vs. RHE). The solid lines correspond to representation of the data according to the equivalent circuit shown in Fig. 3.

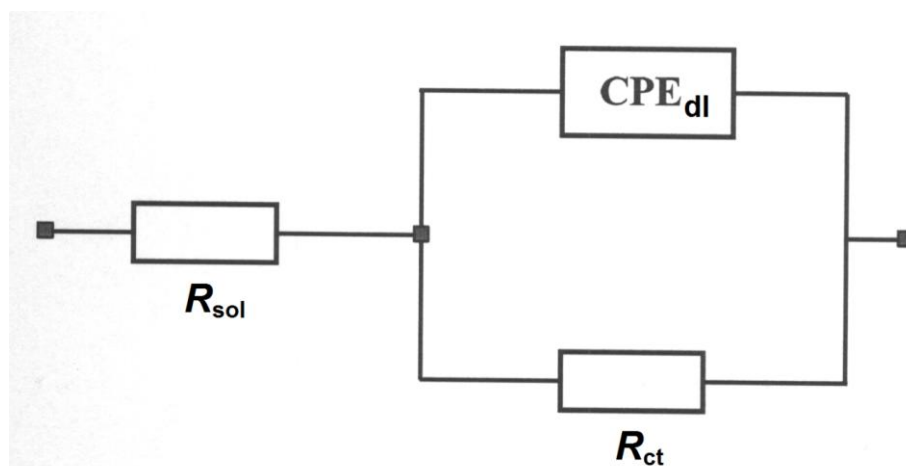


Figure 3. Equivalent circuit model used for fitting the impedance data for 12K CF-based tow electrodes, obtained in 0.1 M NaOH. The circuit includes a constant phase element (CPE) for distributed capacitance; R_{ct} and C_{dl} (CPE_{dl}) elements correspond to the HER charge-transfer resistance and double-layer capacitance components; R_{sol} is solution resistance.

Here, both electrodes exhibited single, “depressed” semicircles (a single-step charge-transfer reaction: contrast to the porous electrode structure impedance characteristics, as observed for NiCCF tow samples in Ref. [14]) at all studied potentials, in the explored frequency range (see examples of Nyquist impedance plots in Fig. 2). Comparison of Faradaic reaction resistance (R_{ct}) and double-layer capacitance (C_{dl}) parameters for the HER at CF_{ox} and Pd-modified CF_{ox} tow electrodes (derived based on a constant phase element – CPE-modified Randles equivalent circuit model shown in Fig. 3) is presented in Table 1. The CPE element was used in the circuit in order to account for the capacitance dispersion effect (represented by distorted semicircles in the Nyquist impedance plots, see Refs. 11-13 and other papers quoted there for details).

Thus, for electrooxidized CF_{ox} electrode the recorded R_{ct} parameter diminished from nearly 40 Ω g at -600 mV to 0.22 Ω g at the potential of -1400 mV vs. RHE (please note however that no significant HER behaviour for the CF_{ox} electrode could be observed, until the potential of -1000 mV vs. RHE was reached, see Fig. 4 below). In addition, it should be stated that for the overpotential range: -50 to -400 mV, the CF_{ox} tow electrode exhibited purely capacitive behaviour (a nearly vertical, 90° line was observed in the Nyquist impedance plots). Then, modification of the CF_{ox} electrode by electrodeposition of ca. 1.5 wt.% of Pd caused a dramatic reduction of the charge-transfer resistance parameter, which came to 1.03 and 0.12 Ω g at the potential values of -50, and -600 mV, respectively. The above translates to the reduction of the R_{ct} parameter by about 330 times, at the potential value of -600 mV (see Table 1 for details).

Furthermore, the double-layer capacitance parameter substantially varied with overpotential. Hence, for the CF_{ox} tow electrode, the C_{dl} rose by ca. 2.6 times, from 109,210 $\mu\text{F g}^{-1}\text{s}^{\phi 1-1}$ at -600 mV to 285,526 $\mu\text{F g}^{-1}\text{s}^{\phi 1-1}$ at -1400 mV vs. RHE. This result is in contrast to the typical HER behaviour observed for the CF-based materials, where the C_{dl} parameter tends to diminish with rising overpotential (see e.g. Refs. 11, 13 and 14 for details). However, dramatically increasing double-layer capacitance upon overpotential augmentation could be explained here in terms of severe surface

inhomogeneity that exists within the complex, 12,000-filament CF tow's entity. In other words, at extended cathodic overpotentials significantly larger area of the tow's electrode becomes available for the HER to proceed.

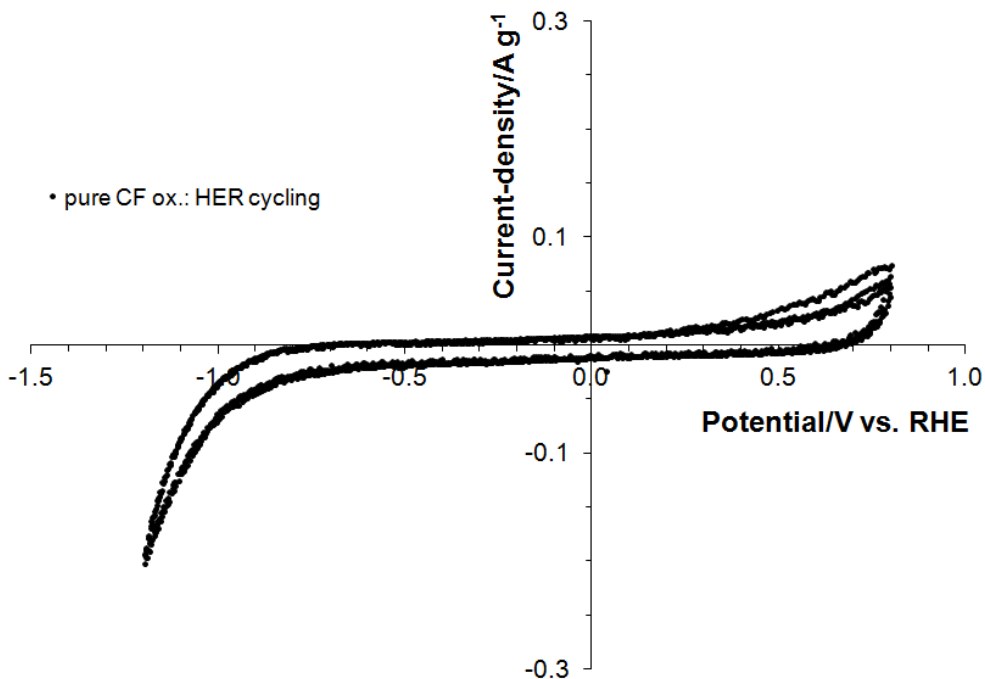


Figure 4. Cyclic voltammograms for electrooxidized Hexcel 12K AS4C CF tow electrode in 0.1 M NaOH, recorded at a sweep rate of 50 mV s^{-1} , including the potential range, where the HER takes place (*HER cycling*) and that for potentials positive to the HER range.

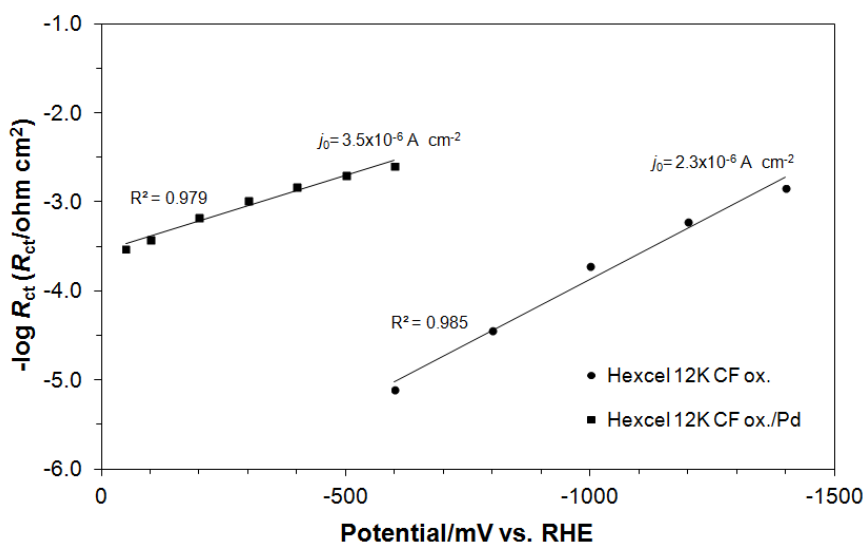


Figure 5. $-\log R_{ct}$ vs. overpotential relationship, obtained for the HER in 0.1 M NaOH solution, for the stated CF-based 12K tow electrodes. Symbols represent experimental results and lines are data fits.

On the other hand, a substantial (relative) increase of the recorded double-layer capacitance for the Pd-modified CF_{ox} electrode (by *ca.* 1.7 times for -600 mV, see Table 1 again) is indicative of significant surface roughening, being a result of electrodeposition of palladium. However, for the Pd-modified fibre electrode the calculated C_{dl} parameter was virtually overpotential independent and oscillated around 180,000-190,000 $\mu\text{F g}^{-1}\text{s}^{\varphi_1-1}$ for the potential range: -50 to -600 mV. This behaviour is in contrast to that observed for the electrooxidized carbon fibre tow electrode and most likely results from the fact that on the palladium-modified fibre electrode the HER proceeds preferentially on the highly active Pd sites, where these are primarily concentrated on the outside layers of the CF filaments. Simultaneously, the dimensionless φ_1 parameter (φ determines the constant phase angle in the complex-plane plot and $0 \leq \varphi \leq 1$) of the CPE circuit (Fig. 3) varied between 0.705 and 0.927.

In addition, a plot of $-\log R_{ct}$ vs. overpotential (see Fig. 5 above) shows a fairly good linear dependence for both examined: CF_{ox} and Pd-modified CF_{ox} electrodes, over the studied overpotential range. This result is in agreement with the kinetically-controlled process [26-29] that proceeds via the Volmer-Heyrovski route (see for instance equations 1 and 2 in Refs. 11-14 and other papers quoted in these works). The exchange current-densities for the HER in Fig. 5 were calculated based on the Butler-Volmer equation and through utilization of the relation between the exchange current-density (j_0) and the R_{ct} parameter for η (overpotential) $\rightarrow 0$ (equation 1):

$$j_0 = \frac{RT}{zFR_{ct}} \quad (1)$$

Thus, the CF-electrooxidized tow electrode exhibited j_0 value of $2.3 \times 10^{-6} \text{ A cm}^{-2}$, whereas for the Pd-modified CF_{ox} sample the recorded exchange current-density came to $3.5 \times 10^{-6} \text{ A cm}^{-2}$. A significant increase of the j_0 parameter (by over 1.5 times) for the latter electrode reflects improvement of catalytic properties towards the HER that is achieved already at very low amount (*ca.* 1.5 wt.%) of electrodeposited Pd element on the activated surface of the carbon fibre tow. Nevertheless, the recorded here exchange current-density value for the Pd-modified CF_{ox} tow electrode was radically lower than that recently derived for an analogous CF sample in 0.5 M H₂SO₄ (compare Fig. 5 below with Fig. 5 of Ref. 14). The above partly results from an existing pH-dependence of the HER characteristics, in addition to rather qualitative nature of employed here electrochemical methods for CF surface electrooxidation, as well as that for Pd electrodeposition, realized at nearly a trace catalyst level.

3.3. Temperature-dependent HER study

Fig. 6 presents $-\log R_{ct}$ vs. T^{-1} (Arrhenius-type) plots, constructed based on the $R_{ct}=f(T)$ a.c. impedance results, presented for the Pd-modified CF_{ox} tow electrode for the overpotential range: -100 through -500 mV (vs. RHE). From the overpotential-dependent slopes of lines shown in Fig. 6, the corresponding, experimental electrochemical energies of activation, E_A [kJ mol^{-1}] for the HER at the CF_{ox}/Pd cathode were also derived and presented in caption to Fig. 6. Hence, the recorded values of E_A parameter expanded from 44.7 kJ mol^{-1} (for -100 mV) to 14.6 kJ mol^{-1} for -500 mV. Interestingly, these results are generally in-line with those recently presented for a commercially available, Toho-

Tenax 12K50 NiCCF (nickel-coated carbon fibre) tow electrode in 30 wt.% KOH supporting electrolyte [12].

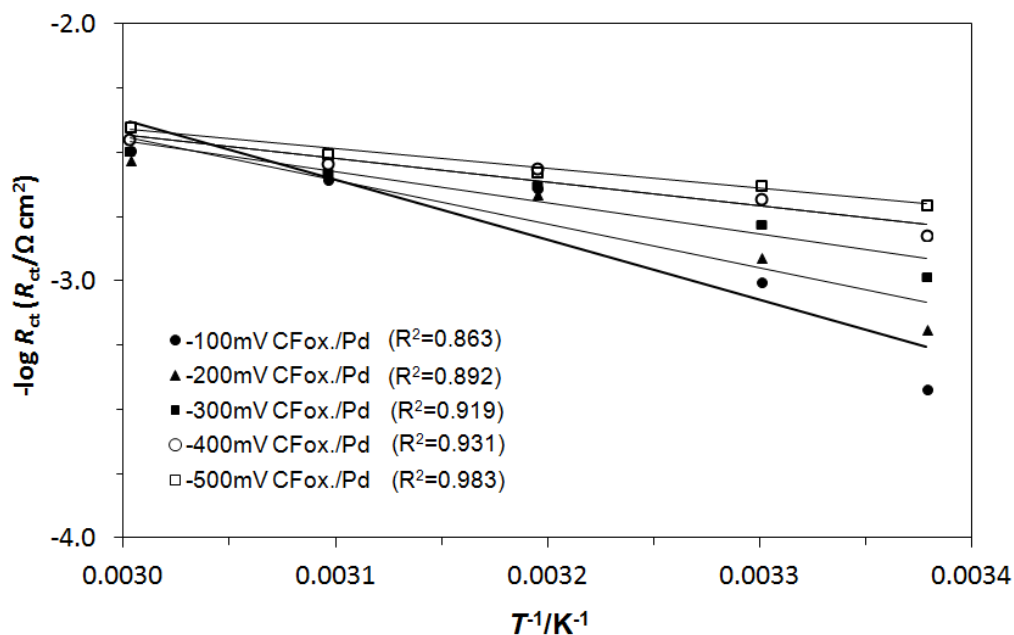


Figure 6. Linear plots of $-\log R_{ct}$ vs. T^{-1} for the HER performed on Pd-modified Hexcel 12K tow electrodes in 0.1 M NaOH solution, at the stated overpotential values; derived electrochemical energies of activation, E_A for a sequence of increasing overpotentials: -100 through -500 mV came to 44.7, 32.5, 23.3, 17.6 and 14.6 kJ mol^{-1} , correspondingly (an appropriate correction was introduced in order to account for a temperature shift of the Pd RHE [30]).

4. CONCLUSIONS

Electrodeposition of palladium at nearly a trace catalyst level (*ca.* 1.5 wt.% Pd) on electrooxidized surface of 12,000-filament carbon fibre tow electrode significantly enhanced catalytic activity of CF_{ox} base material towards cathodic evolution of hydrogen. The above is primarily related to superior catalytic activity of Pd towards hydrogen evolution reaction, in addition to the resultant, substantial extension of electrochemically active surface area of a catalyst material. In addition, both unmodified and Pd-modified CF_{ox} tow entities exhibited electrochemical impedance behaviour with a single, partial semicircle observed in the Nyquist impedance spectra.

As a result, a substantial enhancement of catalytic HER characteristics for a palladium-modified (at very low amount of Pd) CF tow sample, indicates considerable opportunities for this type of cathode materials in commercial water electrolyzers.

References

1. D.D.L. Chung, *J. Mater. Sci.*, 39 (2004) 2645.
2. D. Markham, *Mater. Design*, 21 (2000) 45.

3. S.S. Tzeng and F.Y. Chang, *Mater. Sci. Eng.*, A302 (2001) 258.
4. D.D.L. Chung, *Carbon*, 39 (2001) 279.
5. S.Y. Fu, B. Lauke, E. Mader, C.Y. Yue and X. Hu, *Composites: Part A*, 31 (2000) 1117.
6. J.B. Donnet and R.C. Bansal, *Carbon Fibers*, Marcel Dekker, Inc., New York (1990).
7. M. Mitov, E. Chorbadzhiyska, R. Rashkov and Y. Hubenova, *Int. J. Hydrogen Energy*, doi:10.1016/j.ijhydene.2012.02.102.
8. M.A. Dominguez-Crespo, A.M. Torres-Huerta, B. Brachetti-Sibaja and A. Flores-Vela, *Int. J. Hydrogen Energy*, 36 (2011) 135.
9. M.A. Dominguez-Crespo, E. Ramirez-Meneses, A.M. Torres-Huerta, V. Garibay-Febles and K. Philippot, *Int. J. Hydrogen Energy*, 37 (2012) 4798.
10. R. Solmaz, A. Gundogdu, A. Doner and G. Kardas, *Int. J. Hydrogen Energy*, 37 (2012) 8917.
11. B. Pierozynski and L. Smoczynski, *J. Electrochem. Soc.*, 156(9) (2009) B1045.
12. B. Pierozynski, *Int. J. Electrochem. Sci.*, 6 (2011) 63.
13. B. Pierozynski and T. Mikolajczyk, *Int. J. Electrochem. Sci.*, 7 (2012) 9697.
14. B. Pierozynski, *Int. J. Hydrogen Energy*, 38 (2013) 7733.
15. HexTowTM AS4C Carbon Fiber. Product Data, <http://www.hexcel.com>.
16. J. Barber, S. Morin and B.E. Conway, *J. Electroanal. Chem.*, 446 (1998) 125.
17. J.H. Barber and B.E. Conway, *J. Electroanal. Chem.*, 461 (1999) 80.
18. B.E. Conway and B.V. Tilak, *Electrochim. Acta*, 47 (2002) 3571.
19. A.C.D. Angelo, *Int. J. Hydrogen Energy*, 32 (2007) 542.
20. N.M. Markovic, S.T. Sarraf, H.A. Gasteiger and P.N. Ross, *J. Chem. Soc. Faraday Trans.*, 92 (1996) 3719.
21. J.Y. Huot and L. Brossard, *Int. J. Hydrogen Energy*, 12(12) (1987) 821.
22. H.E.G Rommal and P.J. Morgan, *J. Electrochem. Soc.*, 135(2) (1988) 343.
23. D.M. Soares, O. Teschke and I. Torriani, *J. Electrochem. Soc.*, 139(1) (1992) 98.
24. C. Hitz and A. Lasia, *J. Electroanal. Chem.*, 500 (2001) 213.
25. J.R. Macdonald, *Electrochim. Acta*, 35 (1990) 1483.
26. J.G. Highfield, E. Claude and K. Oguro, *Electrochim. Acta*, 44 (1999) 2805.
27. N. Krstajic, M. Popovic, B. Grgur, M. Vojnovic and D. Sepa, *J. Electroanal. Chem.*, 512 (2001) 16.
28. R.K. Shervedani and A.R. Madram, *Electrochim. Acta*, 53 (2007) 426.
29. S. Martinez, M. Metikos-Hukovic and L. Valek, *J. Mol. Cat. A: Chem.*, 245 (2006) 114.
30. A. Prokopowicz and M. Opallo, *Solid State Ionics*, 157 (2003) 209.